Cell Reports, Volume *43*

Supplemental information

The chemokine Cxcl14 regulates interneuron differentiation in layer I of the somatosensory cortex

Andrew F. Iannone, Gülcan Akgül, Robin Zhang, Sam Wacks, Nisma Hussein, Carmen Ginelly Macias, Alexander Donatelle, Julia M.J. Bauriedel, Cora Wright, Debra Abramov, Megan A. Johnson, Eve-Ellen Govek, Jacqueline Burré, Teresa A. Milner, and Natalia V. De Marco García

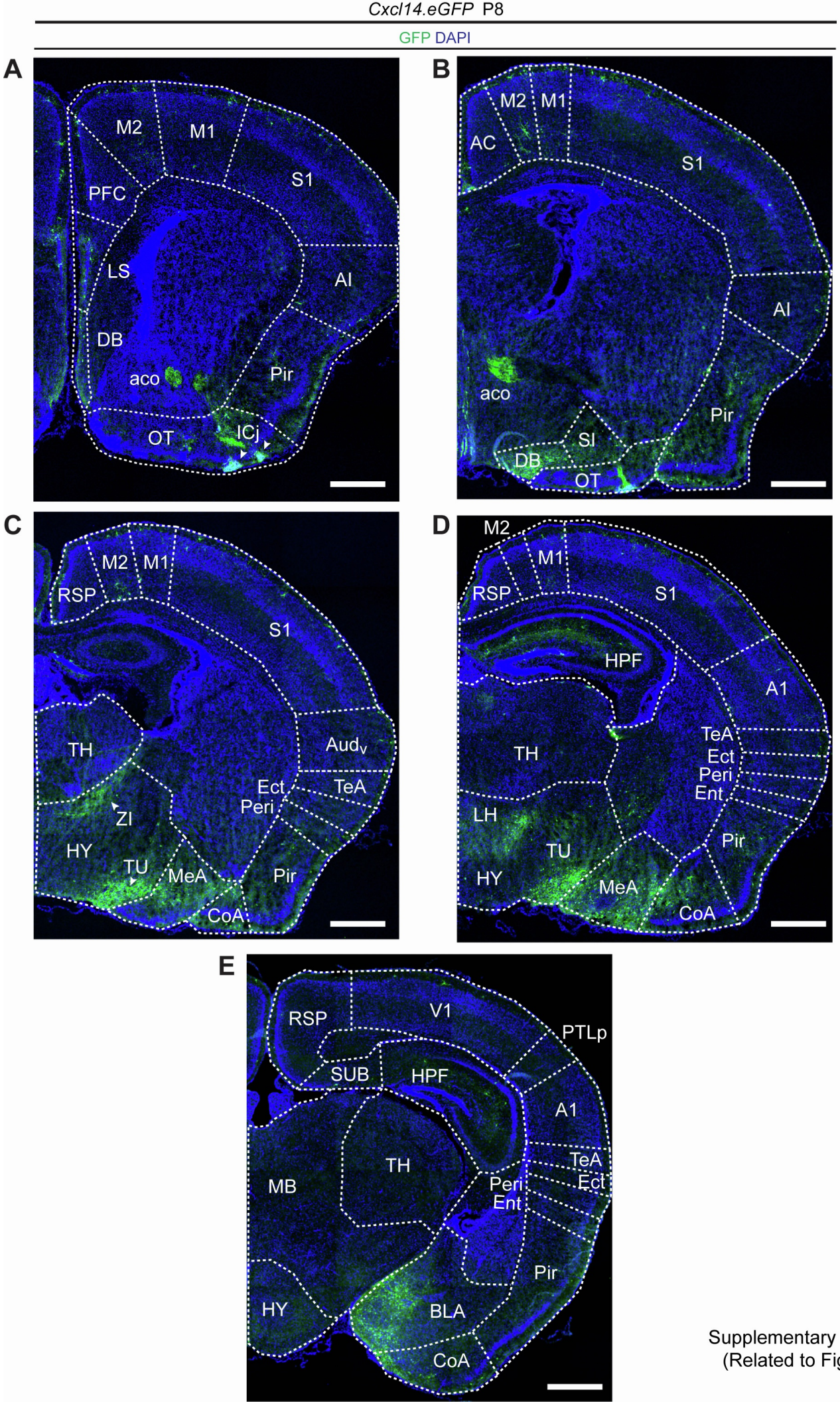

Supplementary Figure 1
(Related to Figure 1)

Figure S1 (related to Figure 1). *Cxcl14.eGFP* expression across cortical regions during development.

(A) *Cxcl14.eGFP* expression is observed in LI at the level of anterior primary somatosensory cortex (S1) and subcortically, in the olfactory tubercle (OT) and Islands of Calleja (ICj), delineated by white arrowheads. aco: anterior commissure; AI: agranular insular areas; DB: diagonal band nucleus; LS: lateral septal nucleus; M1: primary motor cortex; M2: secondary motor cortex; PFC: prefrontal cortex; Pir: piriform area, scale bar 500μm.

(B) Expression of *Cxcl14.eGFP* in the anterior aspect of the somatosensory barrel cortex. AC: anterior cingulate cortex; SI: substantia innominata, scale bar 500μm.

(C) Expression of *Cxcl14.eGFP* in the barrel cortex. Prominent expression is seen in the cortical amygdalar region (CoA) and the medial amygdalar nucleus (MeA). No *Cxcl14.eGFP* expression in somata is detected in thalamic nuclei (TH), while expression in the hypothalamus (HY) is observed in the tuberal nucleus (TU) and zona incerta (IZ), delineated by white arrowheads. Aud_v: ventral auditory area; Ect: ectorhinal area; Peri: perirhinal area; RSP: retrosplenial area; TeA: temporal association areas, scale bar 500μm.

(D) Expression of *Cxcl14.eGFP* at the level of the hippocampal formation (HPF) shows prominent labeling in stratum lacunosum-moleculare of the hippocampal CA1 region. A1: primary auditory cortex; Ent: entorhinal area, scale bar 500μm.

(E) Expression of *Cxcl14.eGFP* at the level of the primary visual cortex (V1). BLA: basolateral amygdalar nucleus; MB: midbrain; PTLp: posterior parietal association areas; SUB: subiculum, scale bar 500μm.

Area labels were determined by aligning images to the reference atlas of the Allen Brain Institute.

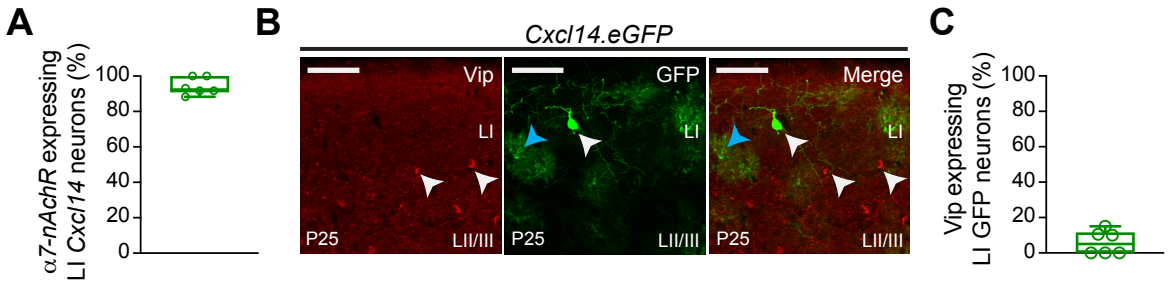

Supplementary Figure 2
(Related to Figure 1)

Figure S2 (Related to Figure 1). Expression of α*7-nAchR* at P8 and Vip at P25 in Layer I Cxcl14 interneurons.

(A) Percentage of cells that co-express α*7-nAchR* and *Cxcl14* over the total number of *Cxcl14* expressing cells in layer (L) I of *Cxcl14.eGFP* mice at P8. n=6 sections from 1 mouse.

(B) Expression of vasoactive intestinal peptide (Vip, left), GFP (middle), and merge (right) in *Cxcl14.eGFP* mice at P25 in LI of S1, scale bar 20μm. White arrowheads delineate neurons that express Vip or GFP, but rarely both. Blue arrowheads demonstrate evidence of GFP expression within astrocytes at P25 (but not at P8; Figure 1A).

(C) Percentage of *Cxcl14.eGFP* expressing neurons that co-express Vip in *Cxcl14.eGFP* mice at P25. n=6 mice.

Data represented as box-and-whisker plots from minimum to maximum range (whiskers) with interquartile ranges (box).

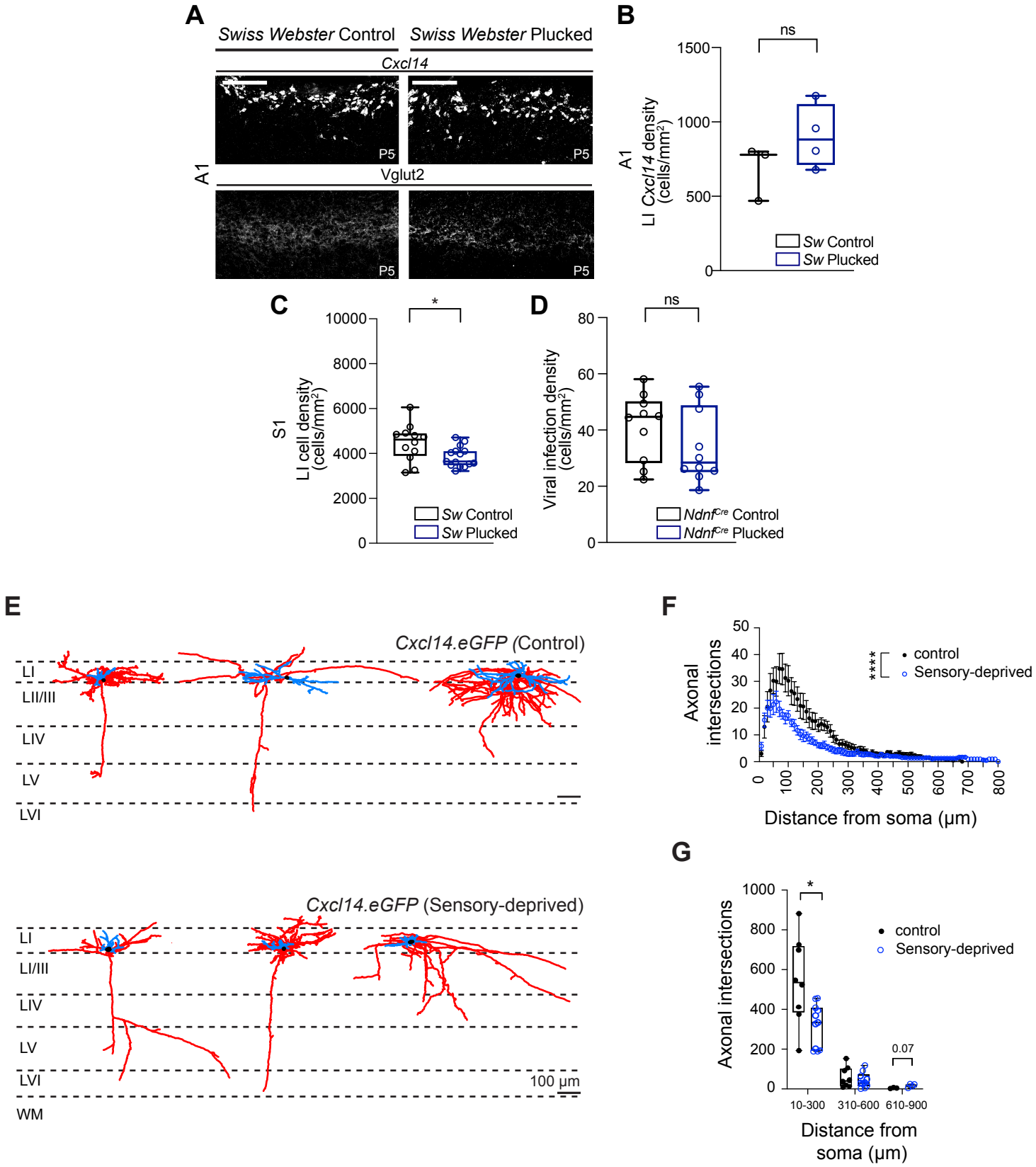

Supplementary Figure 3
(Related to Figure 3)

Figure S3 (related to Figure 3). Whisker plucking does not perturb *Cxcl14* expression in auditory cortex, however, results in morphological changes in *Cxcl14.eGFP* interneurons upon sensory deprivation.

(A) *Cxcl14* expression (top) and Vglut2 immunolabeling (bottom) in *Swiss Webster* (*Sw*) littermate control (left) and daily whisker plucked (right) pups at P5 in primary auditory cortex (A1), scale bars 100μm.

(B) Density of *Cxcl14* expressing cells in *Sw* littermate control and sensory deprived mice at P5 in A1. Unpaired t-test of controls (n=3 sections from 3 mice) vs plucked (n=4 sections from 4 mice): non-significant (ns).

(C) Total density of LI cells, as delineated by DAPI labeling, from *Sw* littermate control and sensory deprived mice at P5 in S1. Unpaired t-test of controls (n=12 sections from 3 mice) vs plucked (n=15 sections from 4 mice): *p = 0.019.

(D) Density of LI neurons in P8 *Ndnf*^{Cre} pups infected with *AAV1-hSyn.FLEx-mGFP-2A-Synaptophysin-mRuby*. Unpaired t-test of controls (n=10 mice) vs daily whisker plucked (n=10 mice): non-significant (ns).

(E) Three representative reconstructions of interneurons with single bouquet cell (SBC) morphology from nontreated (control, top) and whisker-plucked (sensory deprived, bottom) *Cxcl14eGFP* mice at P8-10 in S1. Dashed lines demarcate layer borders (LI, LII/III, LIV, LV, LVI), scale bar 100 μm. Blue: dendrite; red: axon; black: soma.

(F) Scholl analysis for axonal complexity. 2-way ANOVA of control (n=8 cells from 5 mice) versus sensory deprived (n=11 cells from 5 mice): ****p<0.0001.

(G) Axonal intersections in (B) binned as 300 in distance (μm) from soma in versus sensory deprived. Unpaired t-test of control (10-300 μm, n=8 cells; 310-600 μm, n=8; 610-900 μm, n=3) vs sensory deprived (10-300 μm, n=11 cells; 310-600 μm, n=10; 610-900 μm, n=4): *p<0.05.

Data represented as box-and-whisker plots from minimum to maximum range (whiskers) with interquartile ranges (box).

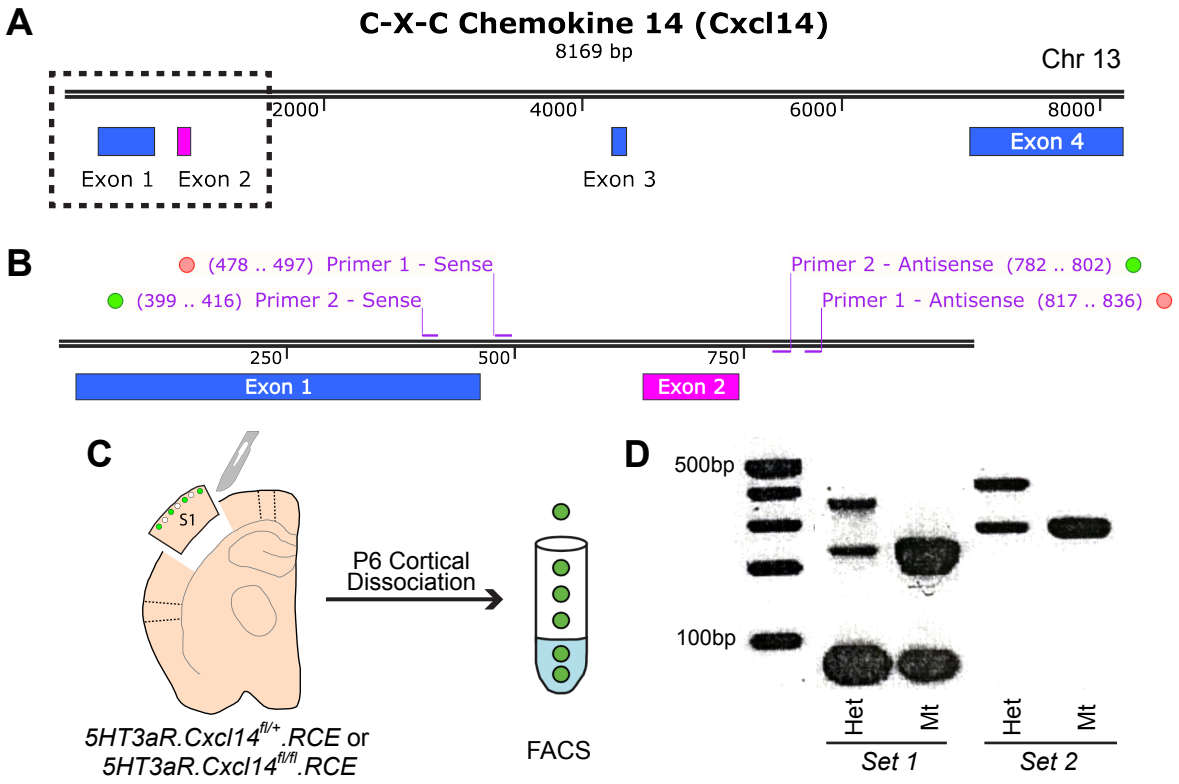

Supplementary Figure 4
(Related to Figure 4)

Figure S4 (related to Figure 4). Effective ablation of *Cxcl14* Exon 2 in *Cxcl14*$^{fl/fl}$ crossed to *5HT3aR.Cre* mice.

(A) Gene map of the *Cxcl14* genetic locus on chromosome (Chr) 13. The locations of the 4 exons in *Cxcl14* mRNA are denoted. The exonic region targeted in *Cxcl14*$^{fl/fl}$ conditional mice is denoted in pink.

(B) Focused gene map for the dotted box area in (A). Genomic locations of two separate primer pairs generated to assess for recombination of exon 2 DNA are indicated.

(C) Schematic of experimental approach to assess for cell-type specific removal via microdissection of primary somatosensory cortex (S1) at P6 followed by fluorescence activated cell sorting (FACS) of GFP expressing neurons.

(D) Representative PCR analysis gel from heterozygous (Het) and mutant (Mt) sorted cells amplified using each distinct primer set denoted in (B). Het: n=3 mice, Mt: n=3 mice. Set 1: floxed band, 325bp, null band, 200bp; Set 2: floxed band, 404bp, null band, 280bp.

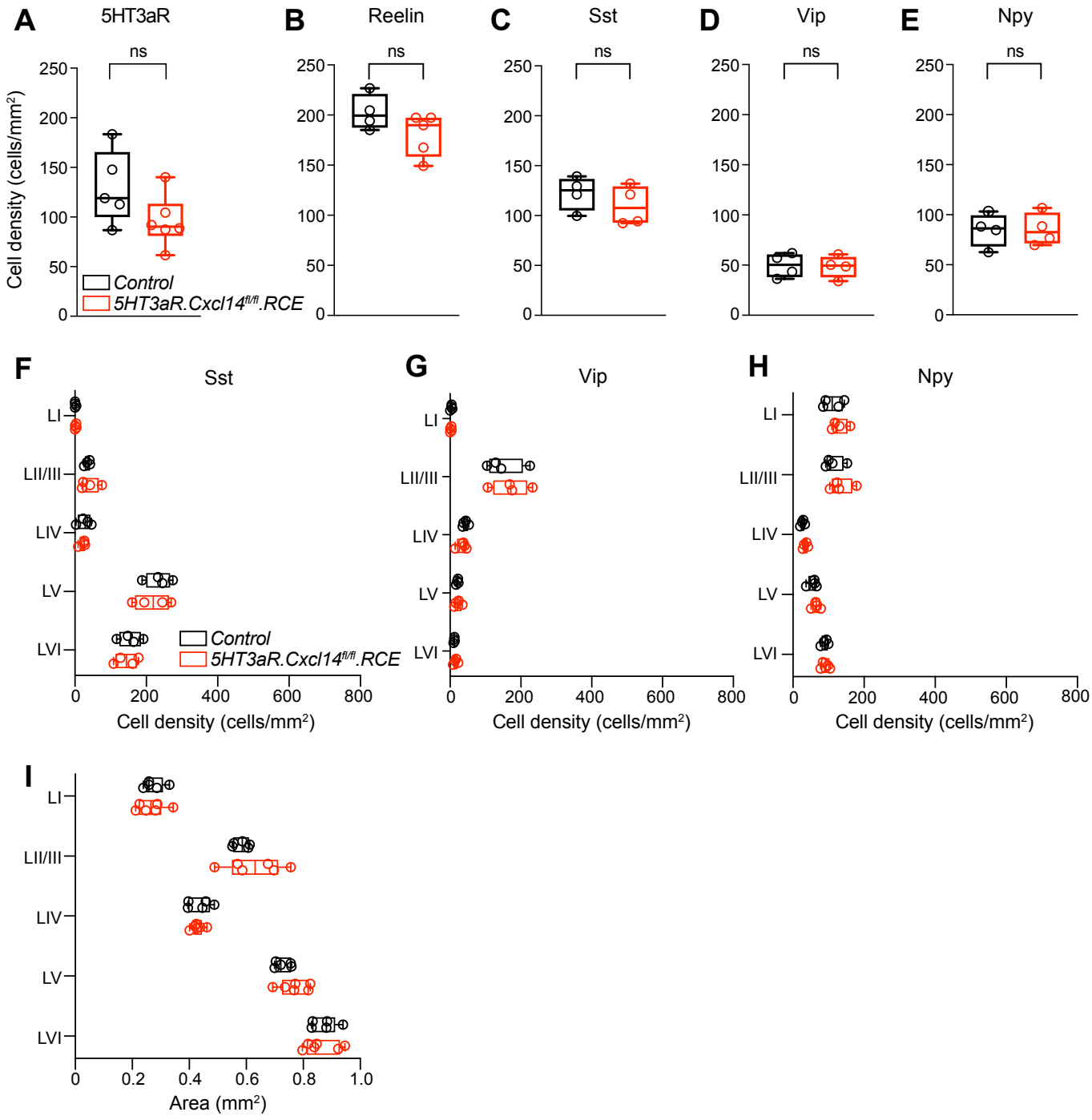

Supplementary Figure 5
(Related to Figure 4)

Figure S5 (related to Figure 4). Interneuron density and lamination are unaffected by developmental loss of *Cxcl14* in CGE-derived interneurons.

(A) Total density of 5HT3aR expressing interneurons as determined by GFP expression in *5HT3aR.RCE* (control, left) and *5HT3aR.Cxcl14$^{fl/fl}$.RCE* (mutant, right) mice at P8 in S1. Unpaired t-test of control (n=5 mice) vs mutant (n=6 mice): non-significant.

(B) Total density of reelin expressing interneurons. Unpaired t-test of control (n=4 mice) vs mutant (n=5 mice): non-significant.

(C) Total density of Sst expressing interneurons. Unpaired t-test of control (n=4 mice) vs mutant (n=4 mice): non-significant.

(D) Total density of vasoactive intestinal peptide (Vip) expressing interneurons. Unpaired t-test of control (n=4 mice) vs mutant (n=4 mice): non-significant.

(E) Total density of neuropeptide Y (Npy) expressing interneurons. Unpaired t-test of control (n=4 mice) vs mutant (n=4 mice): non-significant.

(F) Density by layer of Sst expressing interneurons. 2-way ANOVA with Šidák's multiple comparisons test of control (n=4 mice) vs mutant (n=4 mice) by layer: all genotype comparisons by layer non-significant.

(G) Density by layer of Vip expressing interneurons. 2-way ANOVA with Šidák's multiple comparisons test of control (n=4 mice) vs mutant (n=4 mice) by layer: all genotype comparisons by layer non-significant.

(H) Density by layer of Npy expressing interneurons. 2-way ANOVA with Šidák's multiple comparisons test of control (n=4 mice) vs mutant (n=4 mice) by layer: all genotype comparisons by layer non-significant.

(I) Area of cortical layers as determined by DAPI labeling. 2-way ANOVA with Šidák's multiple comparisons test of control (n=5 mice) vs mutant (n=6 mice) by layer: all genotype comparisons by layer non-significant.

All data represented as box-and-whisker plots from minimum to maximum range (whiskers) with interquartile ranges (box).

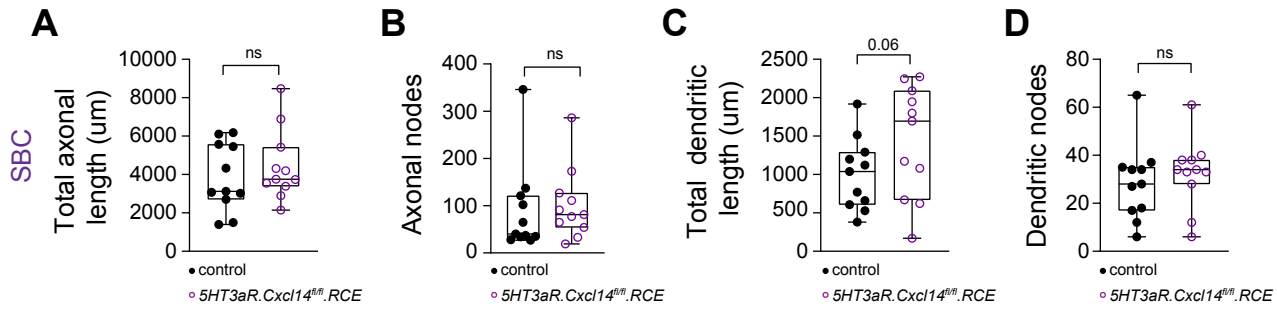

Supplementary Figure 6
(Related to Figure 5)

Figure S6 (related to Figure 5). Impact of *Cxcl14* deletion on LI SBC morphological development.

(A) Total axonal length of single bouquet cells (SBC) from *5HT3aR.RCE* (control) and *5HT3aR.Cxcl14$^{fl/fl}$.RCE* (mutant) mice at P8-10 in S1. Unpaired t-test of control (n=11 cells from 7 mice) vs mutant (n=11 cells from 8 mice): non-significant (ns).

(B) Axonal nodes. Unpaired t-test of control (n=11 cells from 7 mice) vs mutant (n=11 cells from 8 mice): non-significant (ns).

(C) Total dendritic length. Unpaired t-test of control (n=11 cells from 7 mice) vs mutant (n=11 cells from 8 mice): non-significant (ns), p=0.06.

(D) Dendritic nodes. Unpaired t-test of control (n=11 cells from 7 mice) vs mutant (n=11 cells from 8 mice): non-significant (ns).

Data represented as box-and-whisker plots from minimum to maximum range (whiskers) with interquartile range (box).

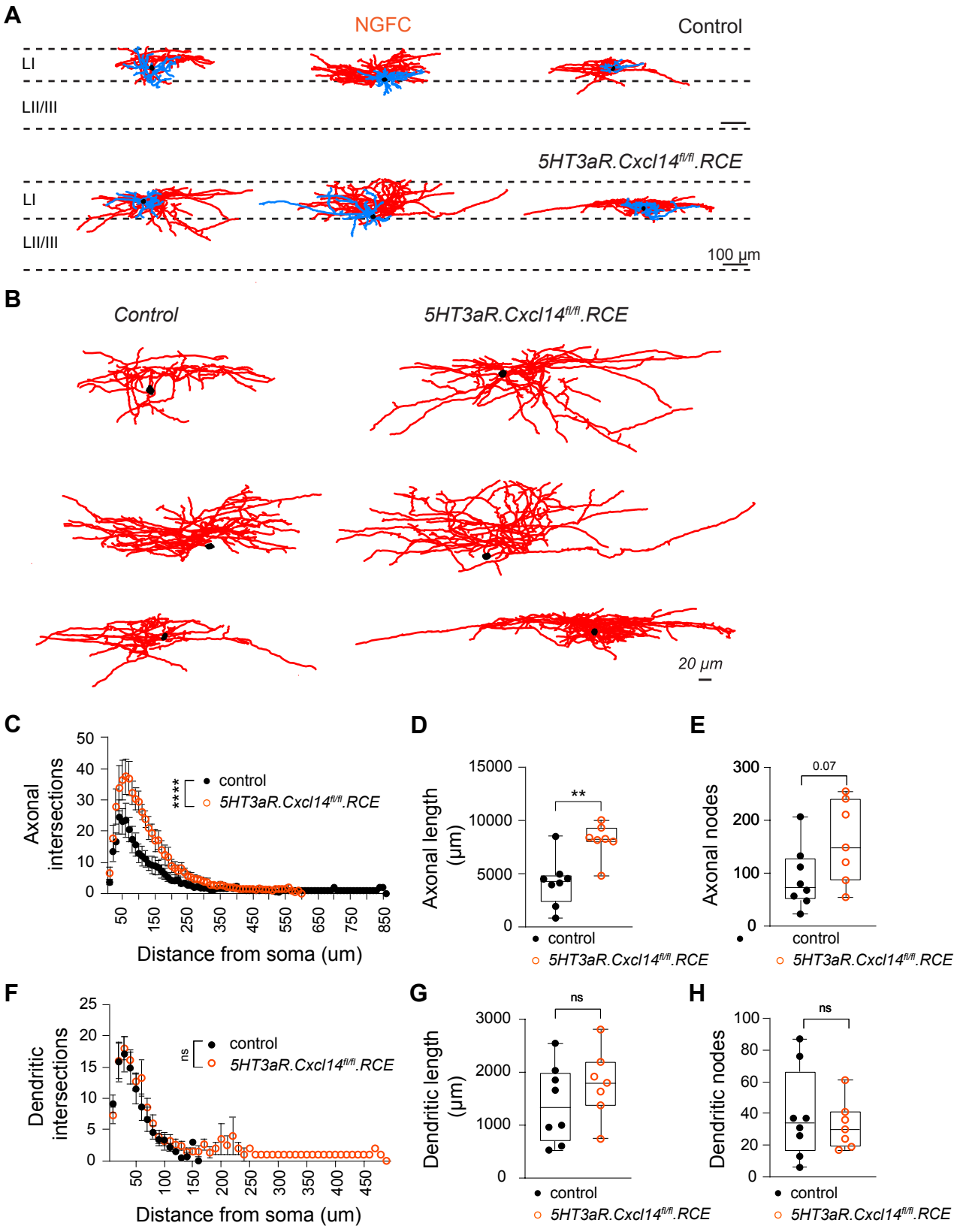

Supplementary Figure 7
(Related to Figure 5)

Figure S7 (Related to Figure 5). LI neurogliaform interneurons exhibit enlarged axonal trees following *Cxcl14* loss.

(A) Three representative reconstructions of neurogliaform (NGFC) interneurons from *5HT3aR.RCE* (control, top) and *5HT3aR.Cxcl14$^{fl/fl}$.RCE* (mutant, bottom) mice at P8-10 in S1. Dashed lines demarcate layer borders (LI, LII/III), scale bar 100 μm. Blue: dendrite; red: axon; black: soma.

(B) High magnification depiction of NGFC axons from *5HT3aR.RCE* (control, left) and *5HT3aR.Cxcl14$^{fl/fl}$.RCE* (mutant, right) mice at P8-10 in S1 as shown in (A), scale bars, 20 μm.

(C) Axonal Scholl analysis. 2-way ANOVA of control (n=8 cells from 7 mice) vs mutant (n=7 cells from 4 mice): ****$p_{genotype}$<0.0001.

(D) Total axonal length. Unpaired t-test of control (n=8 cells from 7 mice) vs mutant (n=7 cells from 4 mice): **p = 0.009.

(E) Axonal nodes. Unpaired t-test of control (n=8 cells from 7 mice) vs mutant (n=7 cells from 4 mice): p = 0.07.

(F) Scholl analysis of dendritic extent. 2-way ANOVA of control (n=8 cells from 7 mice) vs mutant (n=7 cells from 4 mice): non-significant (ns).

(G) Total dendritic length. Unpaired t-test of control (n=8 cells from 7 mice) versus mutant (n=7 cells from 4 mice): non-significant (ns).

(H) Dendritic nodes. Unpaired t-test of control (n=8 cells from 7 mice) versus mutant (n=7 cells from 4 mice): non-significant (ns).

Data represented as box-and-whisker plots from minimum to maximum range (whiskers) with interquartile ranges (box).

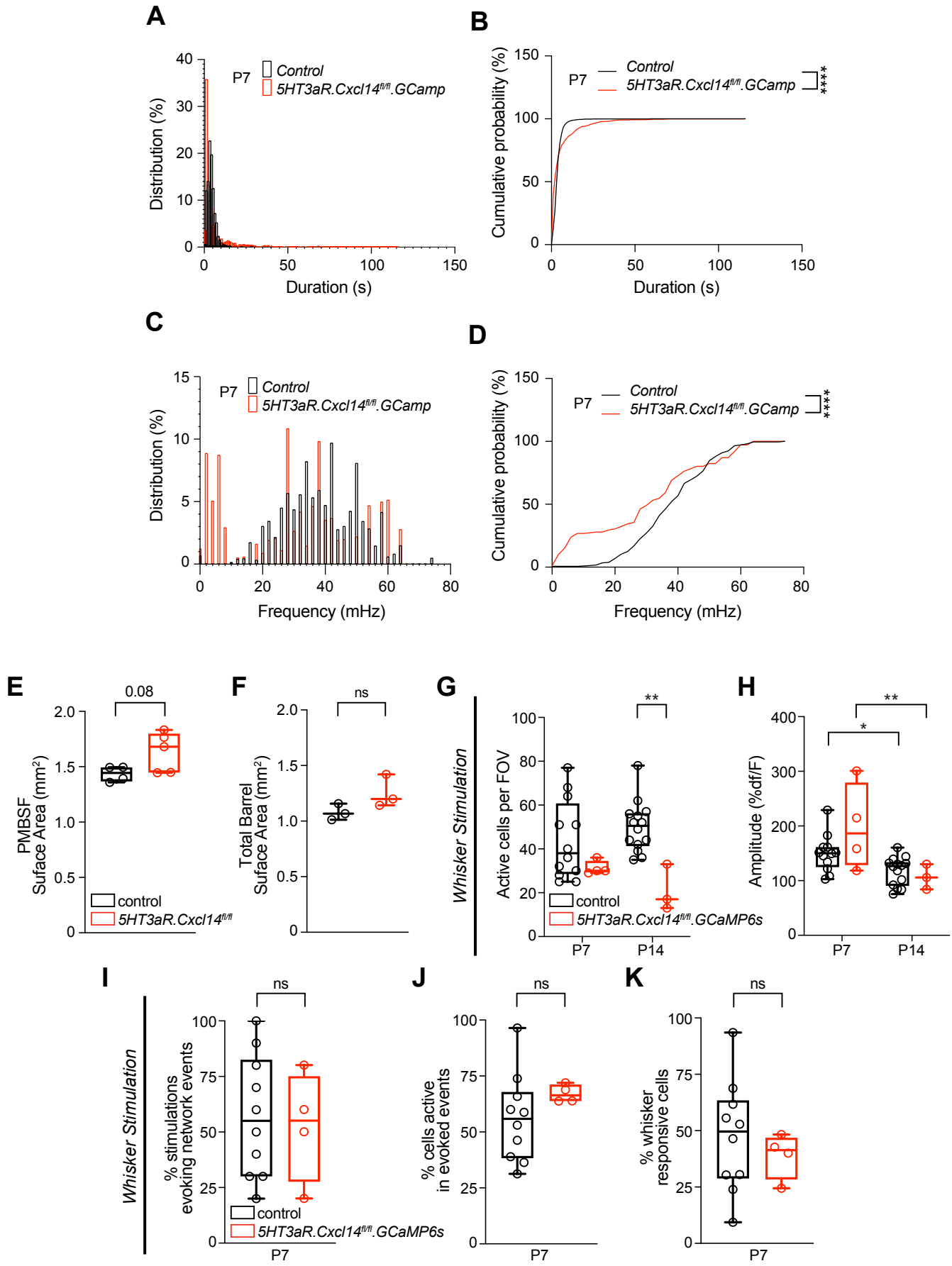

Supplementary Figure 8
(Related to Figure 7)

Figure S8 (related to Figure 7). Developmental impact of *Cxcl14* ablation on cortical networks.

(A) Histogram of the relative duration distribution of single cell calcium events from *5HT3aR.GCaMP6s* (Control, n=12 FOVs from 9 mice) and *5HT3aR.Cxcl14$^{fl/fl}$.GCaMP6s* (KO, n=4 FOVs from 3 mice) at P7, in Figure 7.

(B) Cumulative probability distribution plot of the duration of calcium events from *5HT3aR.GCaMP6* (Control) and *5HT3aR.Cxcl14$^{fl/fl}$.GCaMP6* (KO, n=4 FOVs from 3 mice) at P7, in Figure 7. Kolmogorov-Smirnov test, ****$p < 0.0001$.

(C) Histogram of the relative frequency distribution of calcium events from *5HT3aR.RCE* (Control, n=12 FOVs from 9 mice) and *5HT3aR.Cxcl14$^{fl/fl}$.RCE* (KO) at P7, in Figure 7.

(D) Cumulative probability distribution plot of the frequency of calcium events from 5HT3aR.RCE (Control) and *5HT3aR.Cxcl14$^{fl/fl}$.RCE* (KO) at P7, in Figure 7. Kolmogorov-Smirnov test, ****$p < 0.0001$.

(E) Total surface area of the posteromedial barrel subfield (PMBSF) at P8 in *5HT3aR.Cre* (control) and *5HT3aR.Cxcl14$^{fl/fl}$* (mutant) pups. Unpaired t-test: control (n=4 mice) vs mutant (n=5 mice): non-significant, p=0.076.

(F) Total summed surface area of individual barrels composing the PMBSF (A1-A4, B1-B4, C1-C5, D1-D5, and E1-E5) in *5HT3aR.Cre* (control) and *5HT3aR.Cxcl14* (mutant) pups. Unpaired t-test: control (n=3 mice) vs mutant (n=3 mice): non significant, ns.

(G) Average number of active cells per FOV in *5HT3aR.GCaMP6s* (control, P7: n=12 FOVs from 9 mice; P14: n=14 FOVs from 9 mice) and *5HT3aR.Cxcl14$^{fl/fl}$.GCaMP6s* (mutant, P7: n=4 FOVs from 3 mice; P14: n=3 FOVs from 3 mice) following whisker stimulation. 2-way ANOVA, (**$p_{genotype}<0.01$) followed by Tukey's multiple comparison test: Control vs mutant at P14: **p=0.002.

(H) Average single-cell event amplitude in control (P7: n=12 FOVs from 9 mice; P14: n=14 FOVs from 9 mice) and mutants (P7: n=4 FOVs from 3 mice; P14: n=3 FOVs from 3 mice) following whisker stimulation. 2-way ANOVA (***$p_{age}<0.001$) followed by Tukey's multiple comparisons test: Control P7 vs P14: *p=0.04; Mutant P7 vs P14: **p=0.004.

(I) Average percentage of whisker stimulations that evoked network events in *5HT3aR.GCaMP6s* (control, n=14 FOVs from 10 mice) and *5HT3aR.Cxcl14$^{fl/fl}$.GCaMP6s* (mutant, n=3 FOVs from 3 mice) mice at P7. Unpaired t-test of controls vs mutant: non-significant (ns).

(J) Average percentage of cells active in whisker-evoked network events, normalized to the percentage of total active cells in the FOV in control (n=14 FOVs from 10 mice) and mutant (n=3 FOVs from 3 mice) animals at P7 in S1. Unpaired t-test of control versus mutant: non-significant (ns).

(K) Average percentage of cells responsive to whisker stimulation in control (n=14 FOVs from 10 mice) and mutants (n=3 FOVs from 3 mice) at P7. Unpaired t-test of control versus mutant: non-significant (ns).

Data represented as box-and-whisker plots from minimum to maximum range (whiskers) with interquartile ranges (box).

Parameter	Genotype	Morphology	P8-10	N	Statistical test	P-value
RMP (mV)	*Cxcl14.eGFP*	SBC	-46.8 ± 2.4	9	Unpaired t	0.248
	5HT3aR.RCE	NGFC	-52.5 ± 1.5	8		
Rin (MOhm)	*Cxcl14.eGFP*	SBC	705.0 ± 109.8	9	Mann Whitney	0.038*
	5HT3aR.RCE	NGFC	399.7 ± 53.1	11		
SAG (%)	*Cxcl14.eGFP*	SBC	24.6 ± 5.4	7	Mann Whitney	0.126
	5HT3aR.RCE	NGFC	15.9 ± 5.7	11		
Rheobase (pA)	*Cxcl14.eGFP*	SBC	26.7 ± 7.9	10	Mann Whitney	0.279
	5HT3aR.RCE	NGFC	35.3 ± 7.1	11		
AP Threshold (mV)	*Cxcl14.eGFP*	SBC	-38.3 ± 1.2	10	Unpaired t	0.007**
	5HT3aR.RCE	NGFC	-33.8 ± 0.9	11		
AP Onset (ms)	*Cxcl14.eGFP*	SBC	148.9 ± 26.4	10	Mann Whitney	0.013*
	5HT3aR.RCE	NGFC	422.3 ± 70.2	11		
AP Peak (mV)	*Cxcl14.eGFP*	SBC	18.3 ± 1.9	10	Unpaired t	0.047*
	5HT3aR.RCE	NGFC	25.0 ± 2.4	11		
AP Amplitude (mV)	*Cxcl14.eGFP*	SBC	56.6 ± 1.6	10	Mann Whitney	0.925
	5HT3aR.RCE	NGFC	58.8 ± 2.7	11		
AP Half-width (ms)	*Cxcl14.eGFP*	SBC	1.3 ±0.1	10	Unpaired t	0.327
	5HT3aR.RCE	NGFC	1.2 ± 0.1	11		
AP Rise (ms)	*Cxcl14.eGFP*	SBC	0.5 ± 0.03	10	Unpaired t	0.017*
	5HT3aR.RCE	NGFC	0.4 ± 0.03	11		
AP Decay (ms)	*Cxcl14.eGFP*	SBC	0.9 ± 0.06	10	Unpaired t	0.206
	5HT3aR.RCE	NGFC	0.8 ± 0.03	11		
AHP Amplitude (mV)	*Cxcl14.eGFP*	SBC	6.2 ± 0.7	10	Unpaired t	0.867
	5HT3aR.RCE	NGFC	7.0 ± 1.0	11		

Table S1 (Related to Figure 2): Summary of intrinsic properties recorded from SBCs in *Cxcl14.eGFP* at P8-10 (n = 4 mice) and NGFCs in *5HT3aR.RCE* at P8-10 (n = 6 mice). Data presented as average ± SEM. Red asterisks indicate significance.

Parameters	Genotype	P8-10	N	Statistical test	P-value
RMP (mV)	*Control*	-51.3 ± 1.3	35	Unpaired t	0.141
	5HT3aR.Cxcl14$^{fl/fl}$.RCE	-48.7 ± 1.2	44		
Rin (MOhm)	*Control*	488.4 ± 50.5	50	Mann Whitney	0.038*
	5HT3aR.Cxcl14$^{fl/fl}$.RCE	425.1 ± 42.6	45		
SAG (%)	*Control*	16.7 ± 2.1	50	Mann Whitney	0.534
	5HT3aR.Cxcl14$^{fl/fl}$.RCE	15.9 ± 5.7	47		
Rheobase (pA)	*Control*	34.4 ± 3.4	49	Mann Whitney	0.386
	5HT3aR.Cxcl14$^{fl/fl}$.RCE	38.2 ± 3.8	45		
AP Threshold (mV)	*Control*	-34.9 ± 0.6	49	Mann Whitney	0.035*
	5HT3aR.Cxcl14$^{fl/fl}$.RCE	-36.7 ± 0.6	44		
AP Onset (ms)	*Control*	296.6 ± 29.9	49	Mann Whitney	0.268
	5HT3aR.Cxcl14$^{fl/fl}$.RCE	284.7 ± 39.9	44		
AP Peak (mV)	*Control*	19.6 ± 1.3	48	Unpaired t	0.091
	5HT3aR.Cxcl14$^{fl/fl}$.RCE	22.8 ± 1.3	44		
AP Amplitude (mV)	*Control*	54.5 ± 1.5	48	Mann Whitney	0.063
	5HT3aR.Cxcl14$^{fl/fl}$.RCE	59.5 ± 1.2	44		
AP Half-width (ms)	*Control*	1.13 ± 0.04	48	Mann Whitney	0.281
	5HT3aR.Cxcl14$^{fl/fl}$.RCE	1.09 ± 0.04	44		
AP Rise (ms)	*Control*	0.37 ± 0.01	48	Unpaired t test	0.103
	5HT3aR.Cxcl14$^{fl/fl}$.RCE	0.34 ± 0.02	44		
AP Decay (ms)	*Control*	0.75 ± 0.04	48	Mann Whitney	0.690
	5HT3aR.Cxcl14$^{fl/fl}$.RCE	0.75 ± 0.03	44		
AHP Amplitude (mV)	*Control*	6.18 ± 0.4	48	Unpaired t test	0.013*
	5HT3aR.Cxcl14$^{fl/fl}$.RCE	7.68 ± 0.45	44		

Table S2 (Related to Figure 6): Summary of intrinsic properties recorded from *5HT3aR.RCE* (control) at P8-10 (n = 14 mice) and *5HT3aR.Cxcl14$^{fl/fl}$.RCE* (mutant) at P8-10 (n = 10 mice). Data presented as average ± SEM. Red asterisks indicate significance.

Parameters	Genotype	Morphology	P8-10	N	Statistical test	P-value
RMP (mV)	*Control*	SBC	-52.3 ± 2.7	9	Unpaired t	0.134
	5HT3aR.Cxcl14$^{fl/fl}$.RCE	SBC	-46.4 ± 2.2	9		
Rin (MOhm)	*Control*	SBC	372.1 ± 29.1	11	Mann Whitney	0.555
	5HT3aR.Cxcl14$^{fl/fl}$.RCE	SBC	401.1 ± 74.5	12		
SAG (%)	*Control*	SBC	18.7 ± 4.3	11	Mann Whitney	0.787
	5HT3aR.Cxcl14$^{fl/fl}$.RCE	SBC	23.7 ± 5.1	13		
Rheobase (pA)	*Control*	SBC	32.3 ± 3.9	11	Mann Whitney	0.853
	5HT3aR.Cxcl14$^{fl/fl}$.RCE	SBC	44.0 ± 9.7	13		
AP Threshold (mV)	*Control*	SBC	-34.4 ± 0.9	11	Unpaired t	0.044*
	5HT3aR.Cxcl14$^{fl/fl}$.RCE	SBC	-37.5 ± 1.0	13		
AP Onset (ms)	*Control*	SBC	349.3 ± 69.7	11	Mann Whitney	0.943
	5HT3aR.Cxcl14$^{fl/fl}$.RCE	SBC	347.7 ± 84.0	13		
AP Peak (mV)	*Control*	SBC	19.0 ± 2.2	11	Unpaired t	0.283
	5HT3aR.Cxcl14$^{fl/fl}$.RCE	SBC	23.2 ± 2.7	13		
AP Amplitude (mV)	*Control*	SBC	53.5 ± 2.5	11	Unpaired t	0.058
	5HT3aR.Cxcl14$^{fl/fl}$.RCE	SBC	60.7 ± 2.4	13		
AP Half-width (ms)	*Control*	SBC	1.19 ± 0.08	11	Unpaired t	0.156
	5HT3aR.Cxcl14$^{fl/fl}$.RCE	SBC	1.04 ± 0.06	13		
AP Rise (ms)	*Control*	SBC	0.39 ± 0.03	11	Mann Whitney	0.201
	5HT3aR.Cxcl14$^{fl/fl}$.RCE	SBC	0.32 ± 0.02	13		
AP Decay (ms)	*Control*	SBC	0.76 ± 0.05	11	Unpaired t	0.566
	5HT3aR.Cxcl14$^{fl/fl}$.RCE	SBC	0.72 ± 0.04	13		
AHP Amplitude (mV)	*Control*	SBC	7.23 ± 0.55	11	Welch's t	0.530
	5HT3aR.Cxcl14$^{fl/fl}$.RCE	SBC	8.00 ± 1.03	13		

Table S3 (Related to Figure 6): Summary of intrinsic properties recorded from SBCs in *5HT3aR.RCE* (control) at P8-10 (n = 9 mice) and *5HT3aR.Cxcl14$^{fl/fl}$.RCE* (mutant) at P8-10 (n = 8 mice). Data presented as average ± SEM. Red asterisks indicate significance.

Parameters	Genotype	Morphology	P8-10	N	Statistical test	P-value
RMP (mV)	*Control*	NGFC	-52.5 ± 1.54	8	Unpaired t	0.528
	5HT3aR.Cxcl14$^{fl/fl}$.RCE	NGFC	-50.3 ± 2.42	11		
Rin (MOhm)	*Control*	NGFC	399.7 ± 53.1	11	Mann Whitney	0.699
	5HT3aR.Cxcl14$^{fl/fl}$.RCE	NGFC	346.0 ± 31.7	11		
SAG (%)	*Control*	NGFC	15.9 ± 5.7	11	Mann Whitney	0.699
	5HT3aR.Cxcl14$^{fl/fl}$.RCE	NGFC	15.7 ± 4.8	11		
Rheobase (pA)	*Control*	NGFC	35.3 ± 7.1	11	Mann Whitney	0.427
	5HT3aR.Cxcl14$^{fl/fl}$.RCE	NGFC	38.5 ± 5.3	11		
AP Threshold (mV)	*Control*	NGFC	-33.8 ± 0.9	11	Unpaired t	0.749
	5HT3aR.Cxcl14$^{fl/fl}$.RCE	NGFC	-34.3 ± 1.1	11		
AP Onset (ms)	*Control*	NGFC	422.3 ± 70.2	11	Mann Whitney	0.365
	5HT3aR.Cxcl14$^{fl/fl}$.RCE	NGFC	273.4 ± 72.4	11		
AP Peak (mV)	*Control*	NGFC	25 ± 2.4	11	Unpaired t	0.960
	5HT3aR.Cxcl14$^{fl/fl}$.RCE	NGFC	24.9 ± 2.6	11		
AP Amplitude (mV)	*Control*	NGFC	58.8 ± 2.7	11	Mann Whitney	0.735
	5HT3aR.Cxcl14$^{fl/fl}$.RCE	NGFC	59.2 ± 2.5	11		
AP Half-width (ms)	*Control*	NGFC	1.15 ± 0.06	11	Unpaired t	0.979
	5HT3aR.Cxcl14$^{fl/fl}$.RCE	NGFC	1.15 ± 0.08	11		
AP Rise (ms)	*Control*	NGFC	0.37 ± 0.03	11	Unpaired t	0.557
	5HT3aR.Cxcl14$^{fl/fl}$.RCE	NGFC	0.35 ± 0.02	11		
AP Decay (ms)	*Control*	NGFC	0.76 ± 0.03	11	Welch's t	0.527
	5HT3aR.Cxcl14$^{fl/fl}$.RCE	NGFC	0.81 ± 0.07	11		
AHP Amplitude (mV)	*Control*	NGFC	7.04 ± 1.00	11	Unpaired t	0.758
	5HT3aR.Cxcl14$^{fl/fl}$.RCE	NGFC	7.28 ± 0.68	11		

Table S4 (Related to Figure 6): Summary of intrinsic properties recorded from NGFCs in *5HT3aR.RCE* (control) at P8-10 (n = 6 mice) and *5HT3aR.Cxcl14$^{fl/fl}$.RCE* (mutant) at P8-10 (n = 7 mice). Data presented as average ± SEM. Red asterisks indicate significance.